

# Structural Determinants of the Insulin Receptor-related Receptor Activation by Alkali<sup>\*S</sup>

Received for publication, May 28, 2013, and in revised form, October 1, 2013. Published, JBC Papers in Press, October 11, 2013, DOI 10.1074/jbc.M113.483172

Igor E. Deyev<sup>1</sup>, Alla V. Mitrofanova, Egor S. Zhevlenev, Nikita Radionov, Anastasiya A. Berchatova<sup>2</sup>, Nadezhda V. Popova, Oxana V. Serova, and Alexander G. Petrenko

From the Laboratory of Receptor Cell Biology, Shemyakin-Ovchinnikov Institute of Bioorganic Chemistry Russian Academy of Sciences, 117997 Moscow, Russia

**Background:** The IRR is a member of the insulin receptor family that functions as a sensor of alkaline medium.

**Results:** We have identified key motifs of IRR ectodomain that are involved in alkali sensing.

**Conclusion:** IRR activation by alkali is a complex multipoint process.

**Significance:** Understanding activation of IRR potentially similar to insulin receptor activation.

IRR is a member of the insulin receptor (IR) family that does not have any known agonist of a peptide nature but can be activated by mildly alkaline medium and was thus proposed to function as an extracellular pH sensor. IRR activation by alkali is defined by its N-terminal extracellular region. To reveal key structural elements involved in alkali sensing, we developed an *in vitro* method to quantify activity of IRR and its mutants. Replacing the IRR L1C domains (residues 1–333) or L2 domain (residues 334–462) or both with the homologous fragments of IR reduced the receptor activity to 35, 64, and 7% percent, respectively. Within L1C domains, five amino acid residues (Leu-135, Gly-188, Arg-244, and vicinal His-318 and Lys-319) were identified as IRR-specific by species conservation analysis of the IR family. These residues are exposed and located in junctions between secondary structure folds. The quintuple mutation of these residues to alanine had the same negative effect as the entire L1C domain replacement, whereas none of the single mutations was as effective. Separate mutations of these five residues and of L2 produced partial negative effects that were additive. The pH dependence of cell-expressed mutants (L1C and L2 swap, L2 plus triple LGR mutation, and L2 plus quintuple LGRHK mutation) was shifted toward alkalinity and, in contrast with IRR, did not show significant positive cooperativity. Our data suggest that IRR activation is not based on a single residue deprotonation in the IRR ectodomain but rather involves synergistic conformational changes at multiple points.

Insulin receptor-related receptor is a member of the minifamily of three structurally related receptor tyrosine kinases

\* This work was supported by the Russian Foundation for Basic Research (Grants 10-04-01794-a, 11-04-12151-ofi-m-2011, 12-04-01817-a, 12-04-33190, and 12-04-32099), Basic Sciences to Medicine Program of the Russian Academy of Sciences, and by the President of the Russian Federation (Grant MK-127.2012.4).

<sup>S</sup> This article contains supplemental Figs. S1 and S2.

<sup>1</sup> To whom correspondence should be addressed: Laboratory of Receptor Cell Biology, Inst. of Bioorganic Chemistry, Russian Federation, 117997 Moscow, GSP-7, Ul. Miklukho-Maklaya 16/10, Russia. Tel.: 7-495-335-4177; E-mail: deyeve@ibch.ru.

<sup>2</sup> Supported by Megagrant 220 to Y. Kotelevtsev (Grant 11.G34.31.0032) from the Russian Ministry of Education and Science.

that includes the insulin receptor (IR)<sup>3</sup> and insulin-like growth factor receptor (IGF-IR) (1–4). IRR is not sensitive to insulin and two insulin-like growth factors, IGF-I and IGF-II. Moreover, multiyear studies failed to discover any IRR agonist of the protein or peptide nature. Unexpectedly, recent studies revealed an unusual property of IRR to respond to an increase of extracellular medium pH (5, 6). This finding suggests that the hydroxyl anion may represent a natural agonist of IRR (7). The precise mechanism of the IRR pH sensitivity is not known yet and participation of other ubiquitously present proteins or lipids cannot be excluded.

The physiological importance of IRR as a component of the acid-base homeostasis machinery is supported by complementary *in vitro* and *in vivo* studies (5, 8). First, unlike its ubiquitously distributed homologs IR and IGF-IR, IRR is located in only specific cell sets within some tissues that come in contact with extracorporeal fluids of extreme pH such as kidney, pancreas, and stomach, as reviewed in Ref. 7. Second, in transfected cells, IRR (but not IR or IGF-IR) can be activated by external application of mildly alkaline medium independently of its ionic composition, and this effect is dose-dependent (5). Third, IRR knock-out mice, seemingly healthy under standard environmental conditions, fail to respond properly to an experimentally introduced alkali challenge by kidney secretion of excessive base as bicarbonate (5, 8). Thus, the knock-out animal data provide a strong support that the *in vitro* findings of alkali-dependent IRR activation are physiologically relevant.

It appears that, despite strong amino acid sequence homology, the IRR function and activation mechanism are quite distinct from those of IR and IGF-IR and therefore represent a special interest. Generally, receptor tyrosine kinases are activated due to ligand-induced dimerization followed by autophosphorylation of intracellular catalytic domains (9, 10). In the case of the insulin receptor minifamily, the receptor monomers are predimerized by disulfide bonds, and ligand binding induces a major conformational change that eventually results in the catalytic subunits approaching each other (11, 12). Due to proteolytic processing, mature receptor monomers consist of

<sup>3</sup> The abbreviations used are: IR, insulin receptor; IGF-IR, insulin-like growth factor receptor.

disulfide-linked hydrophilic extracellular  $\alpha$ -subunit and membrane-bound  $\beta$ -subunit with a phosphotyrosine kinase domain (13).

We have previously shown that the pH sensitivity of IRR is defined by its extracellular region, which, similarly to other members of the IR minifamily, contains two leucine-rich repeat domains, named L1 and L2, joined by the cysteine-rich C-domain, and three C-terminal fibronectin type III repeats 1 (FnIII-1, FnIII-2, and FnIII-3) (1, 13, 14). The site of the endogenous cleavage lies within the second FnIII repeat.

The qualitative analysis of IR/IRR chimeras revealed involvement of several extracellular domains in IRR alkali sensing with the primary role of L1C domains (5). To get further insight into the mechanism of IRR activation, we have now developed an *in vitro* assay of IRR autophosphorylation that could be quantitated. By analyzing a set of IR/IRR chimeras and IRR point mutants, we have identified key motifs and amino acid residues involved in IRR alkali sensing and estimated their contribution to IRR activation.

## EXPERIMENTAL PROCEDURES

**IRR/IR Chimeric Receptors and Mutagenesis**—The chimeras of human IRR (GenBank<sup>TM</sup> accession no. NP\_055030) and IR (GenBank<sup>TM</sup> accession nos. BC117172) with full or partial ecto-domain swapping were obtained by cloning using PCR strategy as described in Ref. 5. For generation of additional constructions with point mutations or with tyrosine kinase domain swapping, we used megaprimer PCR approach with mutated oligonucleotides. The following primers were used for generation of TK(N) chimera in the tyrosine kinase domain by megaprimer PCR approach: IRR\_TK\_N2, 5'-GGGAGCAGATCTCGATAATCCGAGAGCTGGGGCAGGGC-3'; IRR\_TK\_N1, 5'-TCTTGAGGTCCCACGGGTCATCAGCTCCATCACCACCA-3'. The following primers were used to generate a TK(C) chimera in the tyrosine kinase domain by megaprimer PCR approach: IRR\_TK\_C2, 5'-TCTGGTCATCATGGAGTAAATGGCTCACGGAGACCTGAAGAG-3'; IRR\_TK\_C1, 5'-CCAAGATGAGGCCAACCTTCACACACATTCTGGACAGCATAAC-3'. The following primers were used to generate a TK chimera in the tyrosine kinase domain by megaprimer PCR approach: IRR\_TK\_N2 - 5'-GGGAGCAGATCTCGATAATCCGAGAGCTGGGGCAGGGC-3'; IRR\_TK\_C1, 5'-CCAAGATGAGGCCAACCTTCACACACATTCTGGACAGCATAAC-3'. The following primers were used to generate mutations in L1C domains of IRR: HK\_to\_AA, 5'-CGGAATCCAGCAGCATATTCTGCGCCGCTGCGAGGGGCTGTGCCCT-3' (contains artificial EcoRI site in IRR sequence); H\_to\_A, 5'-CGGAATCCAGCAGCATAATTCTGCGCCAACCTGCGAGGGGCTGTGCCCT-3'; K\_to\_A, 5'-CGGAATCCAGCAGCATATTCTGCGCCGCTGCGAGGGGCTGTGCCCT-3'; R\_to\_A, 5'-GCAGCCAGCCAGAAGACCCTGCCGCTGTGTAGCTTGCCGC-3'; G\_to\_A, 5'-GGTGTGCTGGGTGTGCTGCCGAGCCCTGTGCCAAGACC-3'; L\_to\_A, 5'-CACACGCACAGCCCCACGCGCCACGGCCCCAAGTGCAGG-3'. Primers HK\_to\_AA, H\_to\_A, and K\_to\_A were used to generate of a double mutant or single mutations in His-318 and Lys-319 with artificial EcoRI, which coded identical IRR sequence, by megaprimer PCR approach.

To generate other mutations in Leu-135, Gly-188, and Arg-244, we used primers L\_to\_A, G\_to\_A, R\_to\_A, by megaprimer PCR approach. The sequences of all constructs were confirmed by DNA sequencing.

**Cell Cultures, Transfections, and Tyrosine Phosphorylation Analysis in Intact Cells**—HEK 293 cells were cultured in DMEM supplemented with 10% fetal bovine serum (Hyclone), 1% penicillin/streptomycin, and 2 mM L-glutamine. HEK 293 cells were transfected by unifactin-56 (Unifect Group, Moscow, Russia), according to the manufacturer's instructions. Confluent monolayers of cells on culture dishes were washed with serum-free F-12 and incubated for 3 h in serum-free F-12 containing 1% penicillin/streptomycin. The cells were further incubated in PBS with 60 mM Tris-HCl of the indicated pH or supplemented with 100 nM insulin for 10 min at room temperature and lysed in the loading SDS-electrophoresis buffer.

**Autophosphorylation in Vitro Assay**—HEK 293 cells were transfected with plasmids encoding IRR or mutant proteins with a C-terminal His<sub>6</sub> tag. In 2 days after transfection, the cells were washed by serum-free F-12 and incubated for 3 h in serum-free F-12 containing 1% penicillin/streptomycin. The cells were then lysed in ice-cold lysis buffer (50 mM Hepes-KOH, pH 7.4, 150 mM NaCl, 1% Triton X-100, and 1 mM PMSF). Cell extracts were centrifuged at 15,000  $\times$  g for 15 min, and the supernatants were incubated with Ni-NTA-agarose (Qiagen) at 4 °C for 90 min. The matrices were further washed three times with the lysis buffer and incubated with cold elution buffer (100 mM Hepes-KOH, pH 7.4, 150 mM NaCl, 100 mM imidazole, 15 mM MgCl<sub>2</sub>, 0.1% Triton X-100, and 1 mM Na<sub>3</sub>VO<sub>4</sub>) at 4 °C for 90 min. Two samples of the eluates (80  $\mu$ l) were supplemented with 20  $\mu$ l of 1 M Tris-HCl, pH 7.1 or 9.1 (at +25 °C), and incubated for 30 min on ice. Furthermore, ATP was added to the final concentration of 100 nM, and eluates were placed at 25 °C for 5 min. To stop autophosphorylation reaction, 5 $\times$  SDS-loading buffer was added.

**Antibodies and Western Blotting**—Rabbit anti-IRR antibodies were raised against the IRR C-terminal cytoplasmic domain (amino acids 961–1297) expressed in bacteria as a GST-fusion protein. The anti-pIRR antibodies were raised against KLH-coupled peptide CGMTRDVPYETDpYpYRKG-GKGL from the activation loop of IRR (5). The lysates and eluates were separated by electrophoresis in 8% SDS-polyacrylamide gel followed by transfer onto ECL-grade nitrocellulose (Amersham Biosciences) as described (15). For detection of phosphorylated IRS-1 and actin, we used rabbit anti-pIRS-1 (Tyr-896) (Sigma) and mouse anti-actin (Chemicon) antibodies. The bound antibodies were detected with anti-rabbit or anti-mouse HRP-conjugated secondary antibodies (Jackson ImmunoResearch Laboratories) following visualization with SuperSignal Chemiluminescent Substrate System (Pierce). For quantitative analysis of the Western blots, Molecular Imager VersaDoc MP4000 (Bio-Rad) was used, together with ImageJ and GraphPad 5 software. Hill plots were made using transform functions in GraphPad software with approximations of saturations signals from the autophosphorylation data.

## Insulin Receptor-related Receptor Activation by Alkali

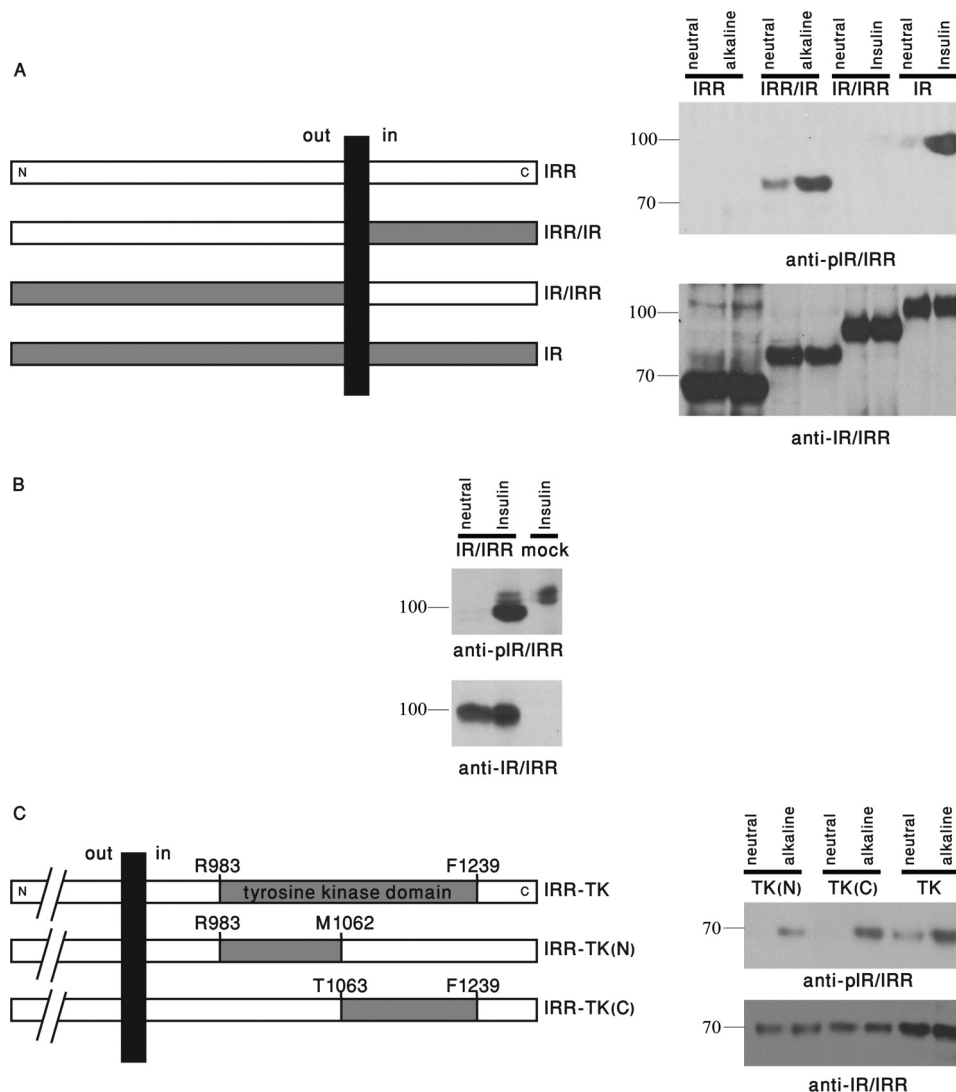


FIGURE 1. *In vitro* phosphorylation of IRR, IR, and their chimeras. *A*, domain models of the His<sub>6</sub>-tagged IR/IRR chimeras (*left panel*). Activation of IR/IRR chimeras by alkali or insulin in the autophosphorylation assay (*right panel*). Transiently expressed chimeras were purified and activated by 200 mM Tris-HCl buffer, pH 7.1 or 9.1, or with addition of 100 nM insulin as described under "Experimental Procedures." Eluted samples were blotted with the indicated antibodies. *B*, activation of the IR/IRR chimera by insulin in intact cells. HEK293 cells were transfected with IR/IRR plasmid and incubated for 10 min in PBS with or without 100 nM insulin. The cells were lysed and blotted with anti-pIR/IRR or anti-IR/IRR antibodies. *C*, domain models of the His<sub>6</sub>-tagged IRR/IR chimeras with full or partial tyrosine kinase domain swapping at the indicated boundaries (*left panel*). Activation of the chimeras by alkali as described in *A* (*right panel*). *Open boxes*, IRR sequences; *filled boxes*, IR. All Western blots shown are representative of at least three independent experiments.

## RESULTS

We have previously determined the role of IRR ectodomain and its fragments in its alkali sensitivity by the analysis of exogenously expressed IR/IRR chimeras (5). The obtained data revealed the involvement of multiple motifs but was qualitative only because the actual amount of surface-expressed receptors was not known. We therefore designed the *in vitro* test system that would allow us to quantify the receptor activation (*i.e.* autophosphorylation) as a function of the ligand concentration. This test was based on the assay performed with immunoprecipitated solubilized insulin receptors (16).

We prepared plasmid constructs encoding C-terminally His<sub>6</sub>-tagged IR and IRR receptors and used them to transfect HEK 293 cells. The expressed proteins were precipitated on Ni-NTA resin and further tested by the *in vitro* autophosphorylation assay. The matrices were incubated in Tris-HCl buffer with

neutral or alkaline pH or with 100 nM insulin and further analyzed by blotting with antibodies against IR/IRR (anti-IR/IRR) and their phosphorylated form (anti-pIR/IRR).

Our preliminary experiments indicated that the *in vitro* autophosphorylation assay worked well for IR but not for IRR. To test the possibility that the identity of intracellular catalytic domain is important for this assay, two chimeras of IRR and IR were prepared (Fig. 1*A*, *left panel*). The first chimera contained the entire extracellular region of IRR fused with the rest of IR (IRR/IR), and the second one contained the entire extracellular region of IR fused with the rest of IRR (IR/IRR). IR and IRR/IR proteins showed strong response to insulin and alkaline medium, respectively (Fig. 1*A*, *right panel*). However, we could not detect any phosphorylation of precipitated IRR and IR/IRR receptors. Essentially, similar results were obtained in the same assay with the addition of 15 mM MnCl<sub>2</sub> to the autophosphor-

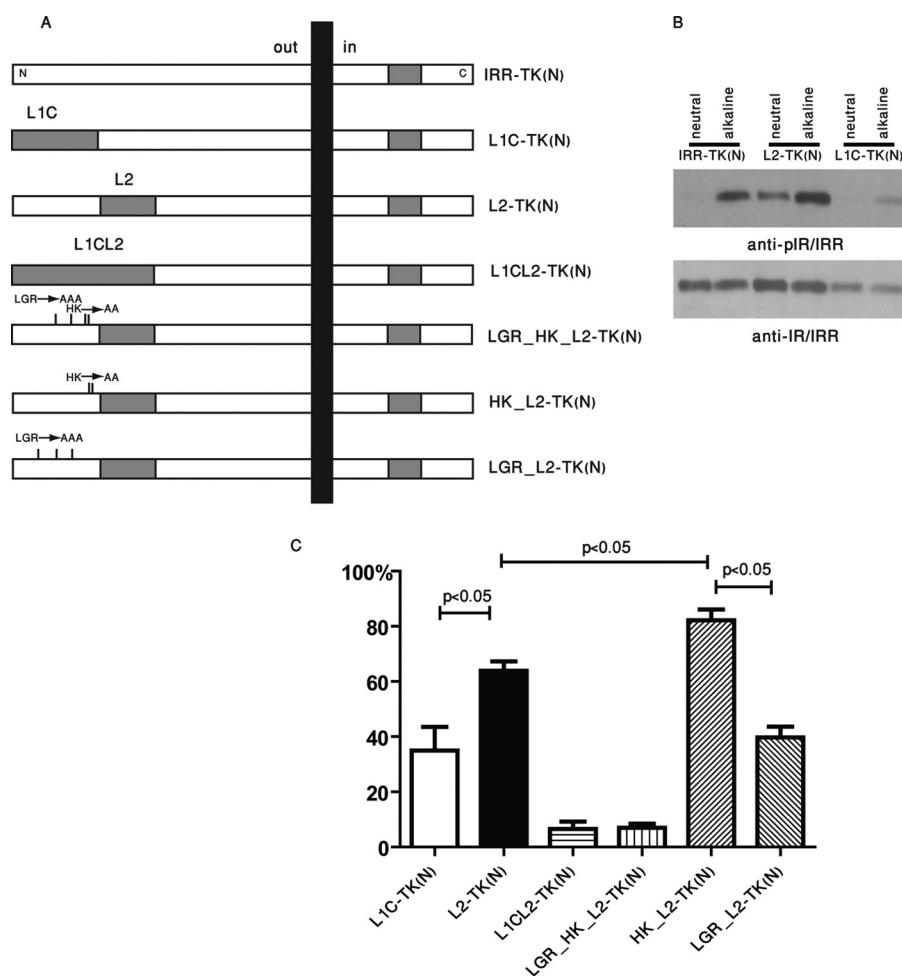


**FIGURE 2. The role of L1C, L2 domains, and the five residues of L1C domains in IRR activation by alkali.** *A*, domain models of the His<sub>6</sub>-tagged L1C and L2 chimeras, and Leu, Gly, Arg, His, and Lys alanine mutants with partial tyrosine kinase domain swapping TK(N), as described in Fig. 1*B*. *Open boxes*, IRR sequences; *filled boxes*, IR. *B*, activation of IRR-TK(N), L1C-TK(N), and L2-TK(N) chimeras by alkali in the *in vitro* autophosphorylation assay. The Western blots were blotted with anti-pIR/IRR antibodies and, after stripping, with anti-IR/IRR antibodies. The shown images are representative of four independent experiments. *C*, quantitative analysis of the activation of the constructs shown in *A* by alkali performed as under "Experimental Procedures." *y* axis values are shown as percentage of IRR-TK(N) activation. Values are means  $\pm$  S.E. ( $n \geq 4$ ).

ylation reaction (data not shown). It should be noted that the IR/IRR construct, similarly to endogenous IR, was autophosphorylated in intact cells upon the insulin treatment (Fig. 1*B*). We also prepared chimeras where only catalytic tyrosine kinase domain or its fragments of IR were introduced into IRR (Fig. 1*C*, *left panel*). The chimera IRR-TK(N) contained the IR fragment from Arg-1027 to Met-1103, the other chimera IRR-TK(C) contained the homologous IR sequence from Thr-1104 to Phe-1283, and the third chimera IRR-TK contained the entire catalytic tyrosine kinase domain (supplemental Fig. S1). The autophosphorylation *in vitro* assay of all three chimeras revealed their response to alkaline medium (Fig. 1*C*, *right panel*). We concluded that this autophosphorylation test could be used to analyze IRR activation but only when its catalytic domain is replaced with the one of IR or its fragments.

Our data are in agreement with the previously reported deficiency of autophosphorylation of yeast-expressed IRR cytoplasmic domain. Under the same conditions, the highly homologous intracellular domains of IR and IGF-IR were autophosphorylated quite well, and the IRR deficiency could be rescued by entire IGF-IR tyrosine kinase domain replacement or just its

C-terminal part (17). The reason of this phenomenon is not clear because the multiple alignment of full IRR, and IR sequences revealed the highest homology precisely within the catalytic tyrosine kinase domain  $\sim 80\%$ . A simple explanation is that the catalytic property is sensitive to the detergent extraction. An alternative possibility is that IRR autophosphorylation in cells requires additional intracellular components such as adaptor proteins or lipids that act as co-factors.

Consequently, all chimeric constructs, tested by *in vitro* phosphorylation assay, included either entire IR catalytic domain or its fragment, depending on expression efficiency of the specific mutant. Three chimeras, containing L1C or L2 domains of IRR, or both substituted with the corresponding sequences of IR, were prepared, and their *in vitro* activity was measured (Fig. 2*A*). To normalize the data for the actual receptor protein amount, the blotting membranes, after staining with anti-pIR/IRR antibodies, were stripped with stripping solution (50 mM Tris-HCl, pH 6.8, 2% (w/v) SDS, 100 mM 2-mercaptoethanol) and reprobed with anti-IR/IRR antibodies (Fig. 2*B*). The differences of normalized phosphosignals after alkaline and neutral pH treatment for L1C-TK(N) or L2-TK(N) chimeras were compared with the same data for IRR-

## Insulin Receptor-related Receptor Activation by Alkali

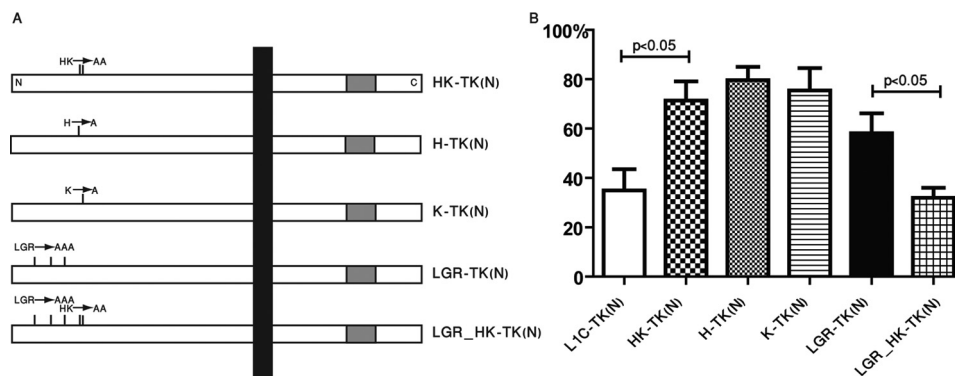


FIGURE 3. **The role of Leu, Gly, Arg, His, and Lys residues within L1C domains.** A, domain models of His<sub>6</sub>-tagged double mutant and single mutants in HK and LGR alanine mutants. *Open boxes*, IRR sequences; *filled boxes*, IR. B, quantitative analysis of the activation of HK-TK(N), H-TK(N), K-TK(N), LGR-TK(N), and LGR\_HK-TK(N) chimeras by alkali in comparison with L1C-TK(N). Values are means  $\pm$  S.E. ( $n \geq 4$ ).

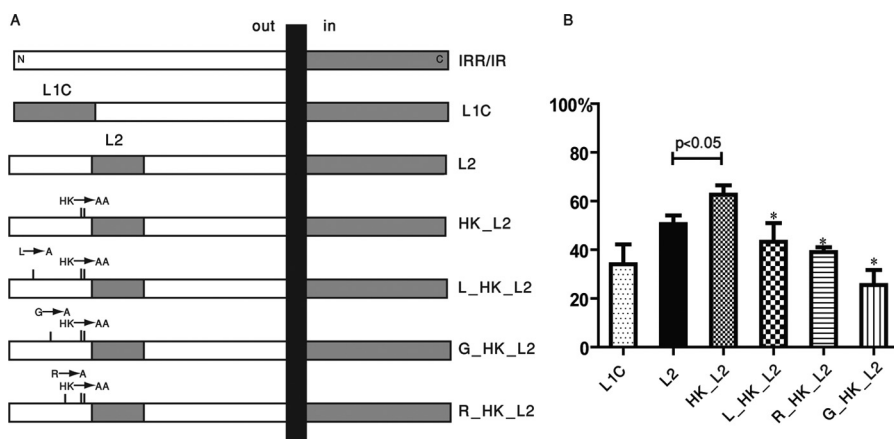


FIGURE 4. **The impact of single Leu, Gly, and Arg mutations on the activity of IRR/IR chimeras.** A, domain models of the His<sub>6</sub>-tagged L2 chimeras with additional mutations in the L1C domains of IRR. B, quantitative analysis of the activation of HK\_L2, L\_HK\_L2, R\_HK\_L2, and G\_HK\_L2 chimeras by alkali in comparison with IRR/IR as 100%. Asterisks indicate  $p < 0.05$  in comparison with the HK chimera. Values are means  $\pm$  S.E. ( $n \geq 4$ ).

TK(N), which was used as the 100% reference. For L1C-TK(N), L2-TK(N), and L1CL2-TK(N) chimeras, we observed a significant reduction of autophosphorylation activity to  $35 \pm 8\%$ ,  $64 \pm 3\%$ , and  $7 \pm 3\%$ , respectively, as compared with chimera with the intact IRR ectodomain (Fig. 2C).

Because L1C substitution produced the strongest effect on IRR sensitivity to alkali, we attempted to identify specific residues in L1C domain that were critically important. We analyzed the multiple alignment of IR, IGF-IR, and IRR sequences from different species (supplemental Fig. S2) by searching for the residues that were conserved in IRR among species but differed significantly from those of IR or IGF-IR, e.g. by polarity or charge. Five amino acid residues in L1C domains of IRR were identified, namely Leu-135 (*versus* Thr in IR and IGF-IR), Gly-188 (*versus* Lys or Met in IR and IGF-IR), Arg-244 (*versus* Thr or Ser in IR and IGF-IR), His-318, and Lys-319 (*versus* TP, IP, or SP in IR and IGF-IR).

To test the importance of the identified amino acid residues for pH sensing, we prepared a set of constructs with all five residues or only some of them mutated to alanine in addition to a swapped L2 domain (Fig. 2A, the *fifth* from above scheme). Alanine mutations are traditionally considered as the least disturbing intervention into the receptor structure. These mutants were expressed at comparable levels and processed correctly. Also, all of them showed some level of the receptor

activity, suggesting there was no serious misfolding problem. The quintuple mutant LGR\_HK\_L2-TK(N) preserved only  $7 \pm 2\%$  of the original full IRR ectodomain construct activity (Fig. 2C). These five mutations appeared to be as effective as the replacement of the entire L1C domains (Fig. 2C). To address the role of specific residues, the activity of constructs with double mutation of two ionic residues His-318 and Lys-319 changed to AA or triple mutation of Leu-135, Gly-188, and Arg-244, together with L2 substitution was further measured (Fig. 2A, the *sixth* and *seventh* from above, respectively). Surprisingly, the HK mutation produced low positive effect on IRR activity, as compared with the L2 chimera. However, the triple LGR mutation decreased the activity to only  $40 \pm 4\%$ , indicating synergism of HK and LGR mutations (Fig. 2C).

Because the HK mutation increased the activity of L2 chimera, a set of similar constructs with also single mutations in His-318 and Lys-319 without L2 swapping was analyzed and compared (Fig. 3A). The HK mutation decreased the activity by  $\sim 29 \pm 8\%$ , whereas single mutations of H or K produced less pronounced effect with activity decrease by  $21 \pm 5\%$  or  $25 \pm 9\%$ , respectively. The triple LGR mutation appeared to be more efficient with  $\sim 42 \pm 8\%$  reduction. The quintuple mutant activity was essentially the same as of L1C chimera (Fig. 3B). We may therefore conclude that the combination of these five amino acid residues play a key role in the L1C pH-sensing machinery.

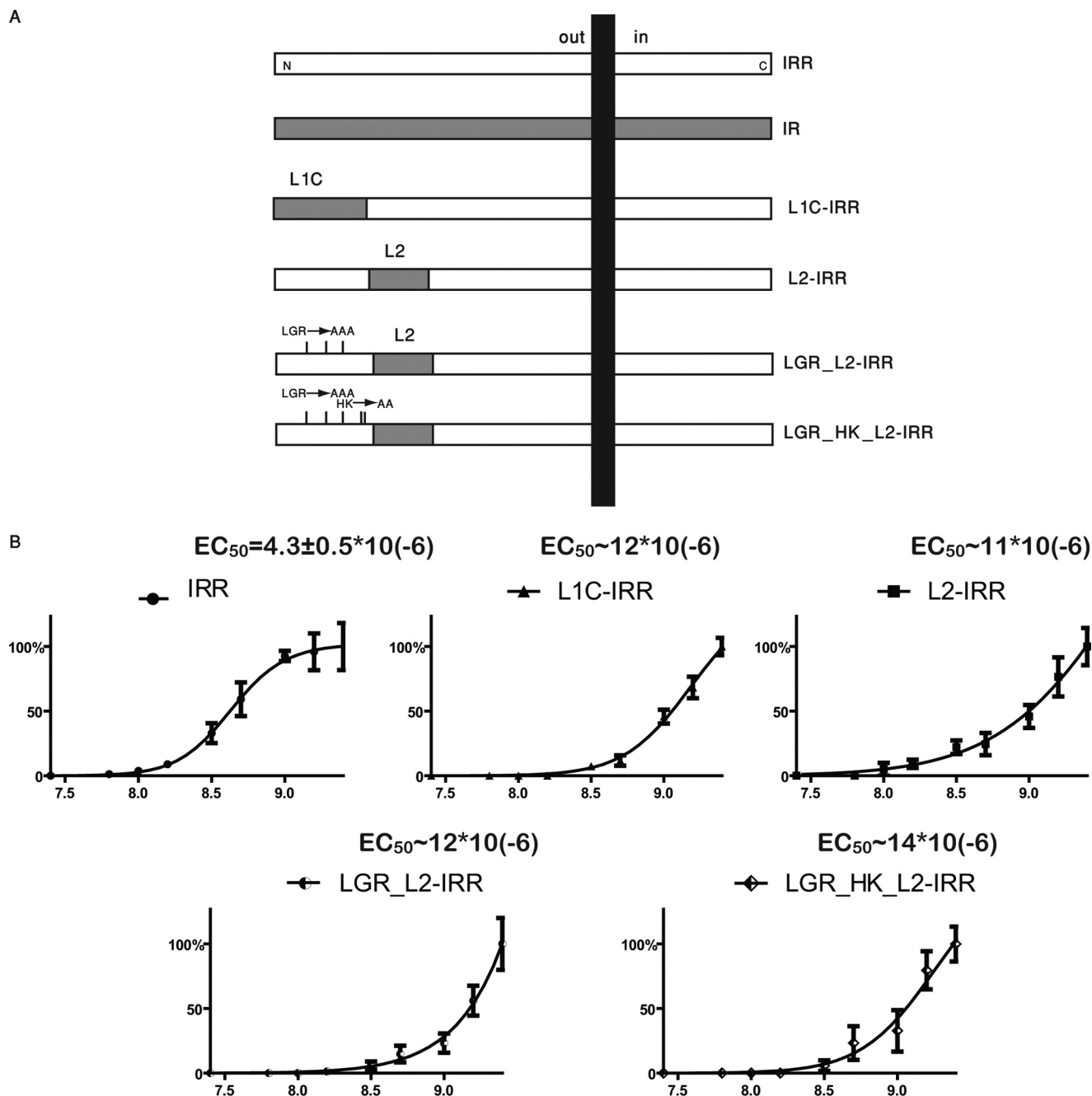


**FIGURE 5. The pH dependence of IRR chimeric mutants.** *A*, domain models of the HA-tagged L1C-IRR and L2-IRR chimeras with additional alanine mutations in the L1C domains of IRR, as indicated. *B*, HEK 293 cells were transfected with indicated plasmids and incubated for 10 min with PBS medium adjusted to the indicated pH by 60 mM Tris-HCl buffer, followed by lysis and blotting with anti-pIR/IRR and anti-IR/IRR antibodies after stripping. Western blot phosphorylation signals were quantified and normalized according to the anti-IR/IRR signals. Phosphosignals were plotted versus pH of the tested solutions. On each plot the y axis shows percentage of the maximum average value of activation at pH 9.4. The values of  $EC_{50}$  were calculated by GraphPad software. Values are means  $\pm$  S.E. ( $n = 4$ ).

We further tested the effect of individual Leu-135, Gly-188, and Arg-244 mutations on the HK and L2 background (Fig. 4A). None of these were critical, Leu-135, Arg-244, or Gly-188 mutations decreased the phosphorylation level of chimeras to  $43 \pm 7\%$ ,  $39 \pm 2\%$ , and  $25 \pm 6\%$ , respectively, with the IRR/IR activity as 100% (Fig. 4B).

To understand the mechanism of the loss of IRR alkali sensing activity in the mutants, we analyzed the pH dependence of their activation. This assay was performed as described previously (5) in live transfected cells to ensure "native" environment

for expressed proteins. All chimeras therefore contained the native intracellular part of IRR. The transfected cells were incubated with a set of Tris-buffered physiological saline solutions with varied pH from 7.4 to 9.4 in small increments. Lysates of transfected cells were directly analyzed by Western blotting with anti-pIR/IRR antibodies and signal quantitation with the Molecular Imager. The blots were further stripped and stained again with anti-IR/IRR C-terminal end antibodies. The ratio of integral density of the phosphorylated receptor (pIR/IRR signal) to the total receptor (IR/IRR antibody signal) was plotted

## Insulin Receptor-related Receptor Activation by Alkali

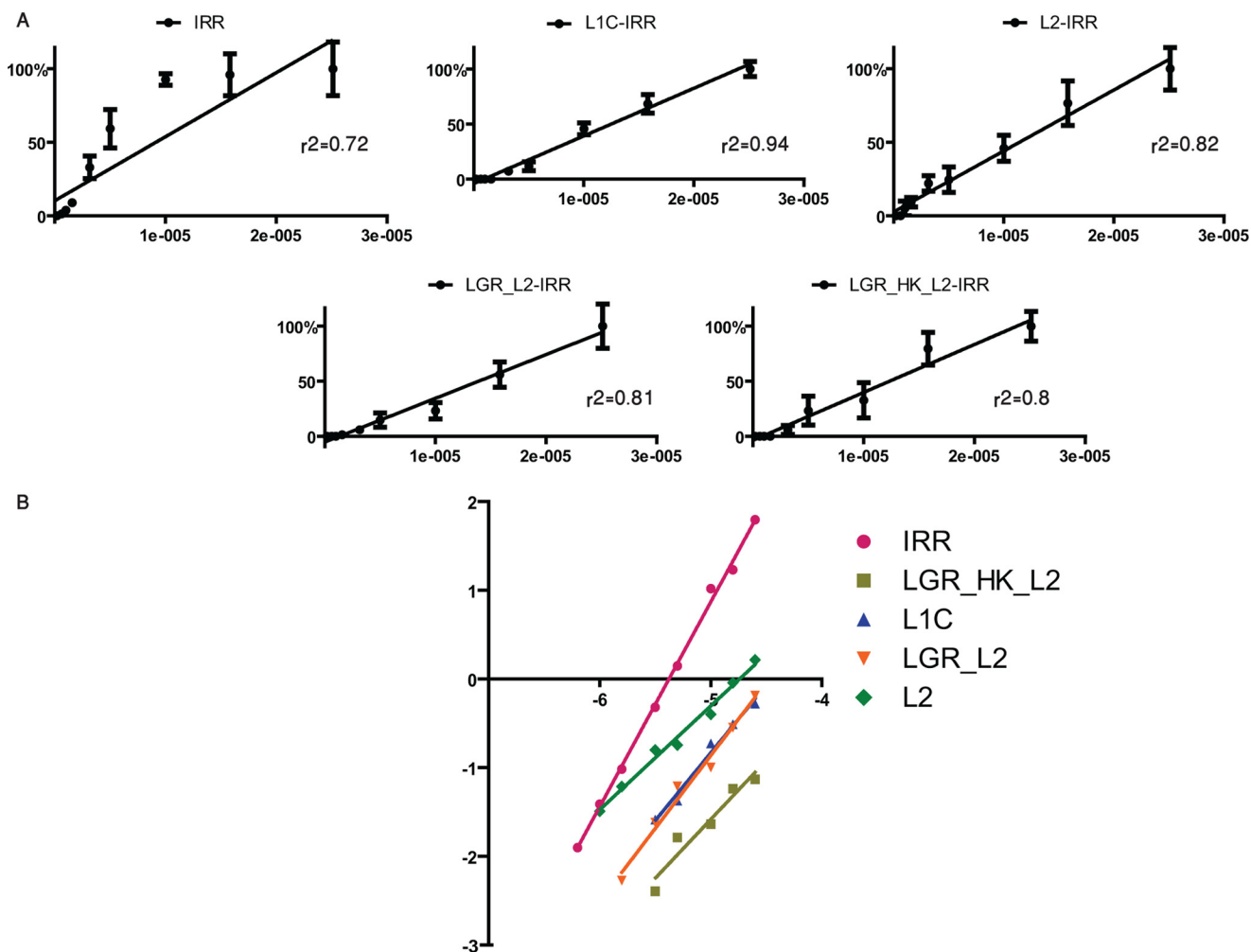


**FIGURE 6. The pH dependence of IRR and its mutant activation (shown in Fig. 5B) in special coordinates.** A, phosphosignals were normalized to the anti-IR/IRR signals and plotted versus hydroxyl ion concentration on a linear scale. On the y axis, the mean value of each mutant activation at pH 9.4 represents 100%. All data were fitted with linear regression by GraphPad software (version 5). The values of  $EC_{50}$  were calculated by GraphPad software (version 5). Values are means  $\pm$  S.E. ( $n = 4$ ). B, Hill plots of mutants activation by alkali. For this analysis, GraphPad software (version 5) was used, and average of replicates for each pH were plotted with linear regression analysis.

versus pH. The effect is shown as percentile of the strongest signal at pH 9.4 for each mutant.

Wild-type IRR together with chimeras L1C-IRR and L2-IRR (5) and two newly constructed chimeras LGR\_L2-IRR and LGR\_HK\_L2-IRR with three or five point mutations in L1C domain of IRR and L2 replacement (Fig. 5A) were analyzed in this test. In the case of wild-type IRR, the activation curve in logarithmic (effect versus pH) coordinates reflected a sharp sigmoid-shaped response with a half effect at pH 8.5–8.6 ( $EC_{50}$ ,  $4.3 \pm 0.5 \mu M$ ), saturation at about pH 9.2, and the Hill slope  $2.3 \pm 0.3$ , as calculated by GraphPad software with nonlinear regression “one site-specific binding with Hill slope” (Fig. 5B). All mutant constructs produced pH dependence curves with a different shape and no signs of saturation were observed (Fig. 5B and see Fig. 6A).  $EC_{50}$  for all tested mutant constructs were shifted toward alkalinity. In linear (effect versus  $[OH^-]$ ) coordinates, all mutants, but not IRR, showed first-order kinetics of their activation that could be fitted by straight lines. The Hill plots with average values for each pH points and each constructs (Fig. 6B) clearly showed higher cooperativity of wild-type IRR activation ( $2.3 \pm 0.1$ ) in comparison with the mutants



**FIGURE 7. IRS-1 phosphorylation by alkali in IRR and L1C/L2 chimera transfected HEK 293 cells.** Cells transfected with indicated plasmids were treated with neutral and alkaline pH. Total lysates of cells were blotted with indicated antibodies. Western blots shown are representative of at least three independent experiments.

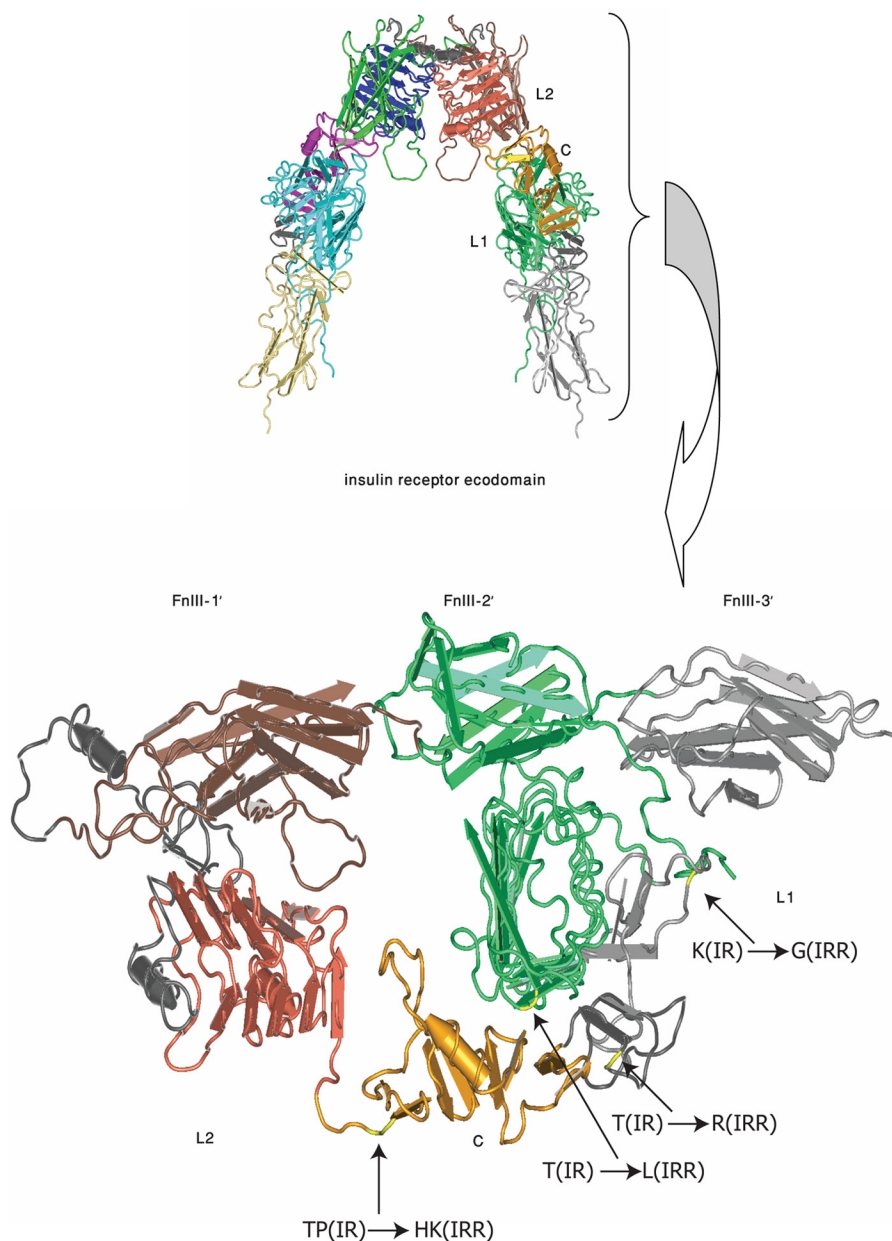


FIGURE 8. Positions of indicated L1, C, and L2 domains, together with Leu-135, Gly-188, Arg-244, His-318, and Lys-319, and their IR substitutes on a putative three-dimensional model of IRR built according to the described structure of IR ectodomain (28) with Cn3D software.

( $1.3 \pm 0.2$  for LGR\_HK\_L2,  $1.5 \pm 0.1$  for LGR\_L2,  $1.6 \pm 0.1$  for L1C, and  $1.2 \pm 0.1$  for L2).

We had previously shown that IRR activation can trigger insulin-like cellular response, in particular, activation of IRS-1. We therefore tested whether significant reduction of the IRR pH-sensing property would also restrain a cellular signaling response. For this purpose, wild-type IRR and its L1CL2 chimera with partial swapping of L1CL2 first three domains of IR with the rest of IRR, that shows only a minor response to alkali treatment (5), were expressed in HEK cells. The cells were treated with F-12 with pH 7.4 or 9.0 adjusted by 60 mM Tris-HCl for 20 min at 37 °C and then lysed and Western blotted with anti-phosphoIRS-1 antibody, with anti-IR/IRR and actin antibodies as controls of IRR expression and protein loading. The resulting data indicated only a minor activation of endog-

enous IRS-1 in the cells expressing the chimera as compared with wild-type IRR-expressing cells (Fig. 7).

## DISCUSSION

The mechanism of IRR activation by alkali is of special interest because of IRR high structural homology with two other members of the IR family. Their activation requires binding of hormone to predimerized receptor subunits followed by a major conformational change eventually leading to autophosphorylation of intracellular kinase domains (18). Yet, the precise mechanism of IR and IGF-IR rearrangement upon ligand binding remains enigmatic. Understanding of hormone-free activation of IRR is of interest as a rare example of pH-induced signaling. It may also shed light on complex events involved in insulin and insulin-like growth factor action.

## Insulin Receptor-related Receptor Activation by Alkali

In this study, we searched for specific differences between IRR and IR that, being relatively minor, generate a unique property of alkali sensing. Previously, we demonstrated that IRR pH sensing is defined by its ectodomain (5). Because IR and IRR have the same domain structure of their extracellular regions, we swapped their large independent fragments and tested the response of chimeras to alkali stimulation in transfected cells. It appeared that essentially all domains of IRR extracellular region were involved in alkali sensing, but their role could not be estimated accurately due to method limitations.

We now developed the *in vitro* assay that allowed us to quantify activity of IRR chimeric mutants with IR swapped domains. We determined that L1C and L2 domains of IRR are most important, their replacement with the corresponding IR fragments decreased IRR activity to ~35 and 64%, respectively (Fig. 2).

We next aimed to identify specific amino acid residues within L1C domains that could be of key importance. By the multiple alignment analysis of the insulin receptor family sequences in several species, five residues in L1C domains were identified that were conserved in species but differed substantially between IRR and IR and IGF-IR, namely Leu-135 (versus Thr in IR and IGF-IR), Gly-188 (versus Lys or Met in IR and IGF-IR), Arg-244 (versus Thr or Ser in IR and IGF-IR), His-318 and Lys-319 (versus TP, IP, or SP in IR and IGF-IR) (Fig. 2 and supplemental Fig. S2).

As the tertiary structure of IRR is not known, the position of these residues can only be predicted within the known crystal structure of IR (Fig. 8). It should be noted that amino acids in the same positions do not map to binding sites for insulin or IGF-I in IR and IGF-IR, which were mapped by mutagenesis scanning approach (supplemental Fig. S2) (19–26) or by crystal structure of contacts between insulin and L1 domain of insulin receptor (27). According to the structure of IR ectodomain, the five mutated residues are not concentrated in a cluster and, most likely, are exposed to the aqueous phase (Fig. 7). Except for Leu-135, they are located in predicted loops between primary folds, raising the possibility that IRR activation involves relative shifts of structural domains. In particular, Lys-319 in IRR would allow higher flexibility of the junction than P in the corresponding position of IR.

Mutation of all the five residues was equivalent to replacement of L1C domains; together with the L2 swapping, it resulted in almost complete loss of the receptor pH sensitivity. The vicinal His-318 and Lys-319 were of special interest since those are ionized residues and thus could be at the heart of the pH sensor. Unexpectedly, His-318/Lys-319 double mutant on the background of the L2 swap showed higher activity (80%) than the L2 swap only chimera, perhaps by relieving structural constraints due to L2 replacement. However, the triple LGR mutation was less potent than the quintuple one. Also, the HK mutation without L2 replacement decreased the receptor activity. Thus, vicinal HK are important for pH sensing but are not likely to be the key pH-sensing residues.

Single residue mutations of Leu-135, Gly-188, and Arg-244 indicate that they all are involved in IRR pH sensing. However, none of these are of critical importance. Their contribution is not precisely additive suggesting they are part of the same

structural component of the IRR activation machinery. The L2 domain is likely to be another independent unit of this mechanism as L2 replacement with the IR L2 domain produces additive effect with point mutations in L1C domains.

To confirm the results of the *in vitro* tests and to determine the pH dependence of the mutant activation, IRR and four mutant constructs (L1C or L2 swap only, L2 plus triple mutation of Leu-135, Gly-188, and Arg-244, and L2 plus quintuple mutation) were transiently expressed and tested in intact cells without receptor solubilization. In contrast with wild-type IRR, the pH sensitivity of all three mutants shifted toward alkalinity, and no saturation was observed at pH values compatible with cell viability. The shape of the pH dependence curves indicated the absence of cooperativity in contrast with strong positive cooperativity of wild-type IRR. Also in intact cells, we showed that the L1C/L2 mutant, in parallel with its low alkaline pH sensitivity, produced very minor IRS-1 activation in contrast with wild-type IRR.

Altogether, our data suggest that IRR activation mechanism is not based on the mere deprotonation of a single residue in a “pH-sensing center” but represents the combination of at least two distinct structural changes that act synergistically. This cooperativity of the conformational change in the IRR ectodomain upon deprotonation may be based, at least partially, on the symmetrical involvement of two IRR subunits that are complexed as a head-to-foot  $\lambda$ -shaped dimer.

## REFERENCES

- Shier, P., and Watt, V. M. (1989) Primary structure of a putative receptor for a ligand of the insulin family. *J. Biol. Chem.* **264**, 14605–14608
- Ullrich, A., Bell, J. R., Chen, E. Y., Herrera, R., Petruzzelli, L. M., Dull, T. J., Gray, A., Coussens, L., Liao, Y. C., and Tsubokawa, M. (1985) Human insulin receptor and its relationship to the tyrosine kinase family of oncogenes. *Nature* **313**, 756–761
- Ullrich, A., Gray, A., Tam, A. W., Yang-Feng, T., Tsubokawa, M., Collins, C., Henzel, W., Le Bon, T., Kathuria, S., and Chen, E. (1986) Insulin-like growth factor I receptor primary structure: comparison with insulin receptor suggests structural determinants that define functional specificity. *EMBO J.* **5**, 2503–2512
- Ebina, Y., Ellis, L., Jarnagin, K., Edery, M., Graf, L., Clauser, E., Ou, J. H., Masiarz, F., Kan, Y. W., and Goldfine, I. D. (1985) The human insulin receptor cDNA: the structural basis for hormone-activated transmembrane signalling. *Cell* **40**, 747–758
- Deyev, I. E., Sohet, F., Vassilenko, K. P., Serova, O. V., Popova, N. V., Zozulya, S. A., Burova, E. B., Houillier, P., Rzhnevsky, D. I., Berchatova, A. A., Murashev, A. N., Chugunov, A. O., Efremov, R. G., Nikol'skiy, N. N., Bertelli, E., Eladari, D., and Petrenko, A. G. (2011) Insulin receptor-related receptor as an extracellular alkali sensor. *Cell Metab.* **13**, 679–689
- Deev, I. E., Vasilenko, K. P., Kurmangaliev, E. Zh., Serova, O. V., Popova, N. V., Galagan, Y. S., Burova, E. B., Zozulya, S. A., Nikol'skii, N. N., and Petrenko, A. G. (2006) Effect of changes in ambient pH on phosphorylation of cellular proteins. *Dokl. Biochem. Biophys.* **408**, 184–187
- Petrenko, A. G., Zozulya, S. A., Deyev, I. E., and Eladari, D. (2013) Insulin receptor-related receptor as an extracellular pH sensor involved in the regulation of acid-base balance. *Biochim. Biophys. Acta* **1834**, 2170–2175
- Deyev, I. E., Rzhnevsky, D. I., Berchatova, A. A., Serova, O. V., Popova, N. V., Murashev, A. N., and Petrenko, A. G. (2011) Deficient Response to Experimentally Induced Alkalosis in Mice with the Inactivated *insrr* Gene. *Acta Naturae* **3**, 114–117
- De Meyts, P. (2004) Insulin and its receptor: structure, function and evolution. *Bioessays* **26**, 1351–1362
- Schlessinger, J. (2000) Cell signaling by receptor tyrosine kinases. *Cell* **103**, 211–225

11. Hubbard, S. R. (1999) Structural analysis of receptor tyrosine kinases. *Prog. Biophys. Mol. Biol.* **71**, 343–358
12. Ward, C. W., and Lawrence, M. C. (2012) Similar but different: ligand-induced activation of the insulin and epidermal growth factor receptor families. *Curr. Opin. Struct. Biol.* **22**, 360–366
13. De Meyts, P. (2008) The insulin receptor: a prototype for dimeric, allosteric membrane receptors? *Trends Biochem. Sci.* **33**, 376–384
14. Bajaj, M., Waterfield, M. D., Schlessinger, J., Taylor, W. R., and Blundell, T. (1987) On the tertiary structure of the extracellular domains of the epidermal growth factor and insulin receptors. *Biochim. Biophys. Acta* **916**, 220–226
15. Deyev, I. E., and Petrenko, A. G. (2010) Regulation of CIRL-1 proteolysis and trafficking. *Biochimie (Paris)* **92**, 418–422
16. Grigorescu, F., White, M. F., and Kahn, C. R. (1983) Insulin binding and insulin-dependent phosphorylation of the insulin receptor solubilized from human erythrocytes. *J. Biol. Chem.* **258**, 13708–13716
17. Klammt, J., Garten, A., Barnikol-Oettler, A., Beck-Sickinger, A. G., and Kiess, W. (2005) Comparative analysis of the signaling capabilities of the insulin receptor-related receptor. *Biochem. Biophys. Res. Commun.* **327**, 557–564
18. Siddle, K., Ursø, B., Niesler, C. A., Cope, D. L., Molina, L., Surinya, K. H., and Soos, M. A. (2001) Specificity in ligand binding and intracellular signalling by insulin and insulin-like growth factor receptors. *Biochem. Soc. Trans.* **29**, 513–525
19. Whittaker, J., Groth, A. V., Mynarcik, D. C., Pluzek, L., Gadsbøll, V. L., and Whittaker, L. J. (2001) Alanine scanning mutagenesis of a type 1 insulin-like growth factor receptor ligand binding site. *J. Biol. Chem.* **276**, 43980–43986
20. Williams, P. F., Mynarcik, D. C., Yu, G. Q., and Whittaker, J. (1995) Mapping of an NH<sub>2</sub>-terminal ligand binding site of the insulin receptor by alanine scanning mutagenesis. *J. Biol. Chem.* **270**, 3012–3016
21. Whittaker, J., Sørensen, H., Gadsbøll, V. L., and Hinrichsen, J. (2002) Comparison of the functional insulin binding epitopes of the A and B isoforms of the insulin receptor. *J. Biol. Chem.* **277**, 47380–47384
22. Mynarcik, D. C., Williams, P. F., Schaffer, L., Yu, G. Q., and Whittaker, J. (1997) Analog binding properties of insulin receptor mutants. Identification of amino acids interacting with the COOH terminus of the B-chain of the insulin molecule. *J. Biol. Chem.* **272**, 2077–2081
23. Rouard, M., Bass, J., Grigorescu, F., Garrett, T. P., Ward, C. W., Lipkind, G., Jaffiole, C., Steiner, D. F., and Bell, G. I. (1999) Congenital insulin resistance associated with a conformational alteration in a conserved  $\beta$ -sheet in the insulin receptor L1 domain. *J. Biol. Chem.* **274**, 18487–18491
24. Nakae, J., Morioka, H., Ohtsuka, E., and Fujieda, K. (1995) Replacements of leucine 87 in human insulin receptor alter affinity for insulin. *J. Biol. Chem.* **270**, 22017–22022
25. Schumacher, R., Mosthaf, L., Schlessinger, J., Brandenburg, D., and Ullrich, A. (1991) Insulin and insulin-like growth factor-1 binding specificity is determined by distinct regions of their cognate receptors. *J. Biol. Chem.* **266**, 19288–19295
26. Rentería, M. E., Gandhi, N. S., Vinuesa, P., Helmerhorst, E., and Mancera, R. L. (2008) A comparative structural bioinformatics analysis of the insulin receptor family ectodomain based on phylogenetic information. *PLoS One* **3**, e3667
27. Menting, J. G., Whittaker, J., Margetts, M. B., Whittaker, L. J., Kong, G. K., Smith, B. J., Watson, C. J., Záková, L., Kletviková, E., Jiráček, J., Chan, S. J., Steiner, D. F., Dodson, G. G., Brzozowski, A. M., Weiss, M. A., Ward, C. W., and Lawrence, M. C. (2013) How insulin engages its primary binding site on the insulin receptor. *Nature* **493**, 241–245
28. McKern, N. M., Lawrence, M. C., Streltsov, V. A., Lou, M. Z., Adams, T. E., Lovrecz, G. O., Elleman, T. C., Richards, K. M., Bentley, J. D., Pilling, P. A., Hoynes, P. A., Cartledge, K. A., Pham, T. M., Lewis, J. L., Sankovich, S. E., Stoichevska, V., Da Silva, E., Robinson, C. P., Frenkel, M. J., Sparrow, L. G., Fernley, R. T., Epa, V. C., and Ward, C. W. (2006) Structure of the insulin receptor ectodomain reveals a folded-over conformation. *Nature* **443**, 218–221